TECHNICAL MEMORANDUM

234

On spurious chaotic behaviour in the discretized ECMWF physics scheme

P.A.E.M. Janssen and J.D. Doyle

Research Department

April 1997

European Centre for Medium-Range Weather Forecasts
Europäisches Zentrum für mittelfristige Wettervorhersage
Centre européen pour les prévisions météorologiques à moyen

ON SPURIOUS CHAOTIC BEHAVIOUR IN THE DISCRETIZED ECMWF PHYSICS SCHEME

Peter A E M Janssen and James D Doyle

1. INTRODUCTION

Some time ago an inconsistency between surface wind and stress was discovered in the ECMWF atmospheric model. The inconsistency was resolved by *Janssen et al.* (1992) who noted that the atmospheric model's time-split scheme which treated physics and dynamics separately, had a time step dependent equilibrium. An implicit treatment of both physics and dynamics removes this deficiency. When the semi-Lagrangian scheme is used, longer time steps are allowed and the use of the semi-split scheme would have further enhanced the consistency between surface wind and stress. The new implicit integration scheme (applied to velocity, temperature and moisture) was therefore introduced with the semi-Lagrangian T213 version of the ECMWF model (*Ritchie et al.*, 1995). Although this semi-implicit treatment of physics and dynamics gives proper steady states, there is no guarantee that in rapidly varying circumstances the implicit scheme is accurate. This is illustrated by Fig 1 where we have plotted from a simulation with the T213 version of the ECMWF model the simulated drag coefficient versus wind speed at 31 m height over the oceans. The roughness length is given by the Charnock relation and the resulting drag coefficient as function of wind speed for neutral stratification is shown as the full line in Fig 1. For high winds, corresponding to a low level jet associated with a rapidly developing cyclone case in the North Sea, the simulated drag coefficient is too low, suggesting the above mentioned inconsistency.

Since the introduction of the prognostic cloud scheme, oscillations can appear rather frequently in quantities such as the heat flux. An example from the single grid point model is shown in Fig 2. Initial conditions for this run were obtained from profiles of a grid point at sea of the atmospheric model, and in Fig 2 the time evolution of the heat flux is presented for a layer just above a layer with clouds. The almost quasi periodic behaviour of the heat flux is of course an undesirable property of the atmospheric model. Even the time averaged heat flux is not correct, since the exact' solution (shown as the grey line) gives, in this case, a systematically higher flux.

All this prompted a renewed interest in the properties of the ECMWF integration scheme for physical processes. The study of the complete ECMWF physics scheme was thought to be too complicated and therefore Section 2 is devoted to an analysis of a simple one-dimensional evolution equation which reflects a relevant physical problem. Results from this example suggest that as long as a physical process has a short time scale and is sufficiently nonlinear, its discretised implementation will have the properties described below. Discretising the continuous equation results in studying the properties of a one-dimensional map $x_{n+1} = f(x_n, \lambda)$, where x_n is the relevant variable at time level n and λ is a parameter which is in essence the time step of the

numerical scheme. The one-dimensional map and its properties have been studied extensively in the context of chaos (*Feigenbaum*, 1980). We assume that the time-continuous problem has at least one stable fixed point. For small enough values of the bifurcation parameter also in the discretised equation the fixed point is stable. However, depending on the degree of nonlinearity of, for example, the turbulent fluxes the fixed point becomes unstable at the critical value λ_1. Beyond the critical value the solution starts to oscillate with period 2 ($\times \Delta t$). Increasing the bifurcation parameter further, the period 2 oscillation becomes unstable at the critical value λ_2 and for $\lambda > \lambda_2$ we have another period doubling. This process of successive period doubling continues with the range of parameter (λ) values for which the period remains fixed, becoming smaller and smaller until, at a certain value of the bifurcation parameter λ, it has doubled ad infinitum so that the behaviour is no longer periodic. This is one of the routes to chaotic behaviour but since the continuous system does not have chaos (it has a single stable fixed point) the chaotic behaviour of the numerical scheme may be regarded as spurious and should therefore be avoided. However, our analysis does provide an explanation for the noise in a number of physical quantities in the ECMWF physics.

It is clear that one should introduce a numerical scheme that avoids the above-mentioned spurious aperiodic behaviour and a secure way to do this is to use a scheme that always has a stable fixed point (section 3). A practical scheme which meets this requirement is the linearised Crank-Nicholson scheme. However, this scheme requires the tangent linear of both Physics and Dynamics which is presently not available. We also discuss the idea to call the physics subroutines (i.e. *Vdiff*) n times with a time step $\Delta t/n$. Although this approach does not guarantee a stable fixed point, it makes it more unlikely that instability occurs. Moreover, the iteration approach may be readily implemented in the framework of the ECMWF atmospheric model. The iteration scheme is successfully applied to the low level jet case and it removes oscillations in the heat flux.

In Section 4 we introduce the iteration scheme into the atmospheric model and discuss its impact on wind field and pressure field of the record low of January 10 1993. Also results of 12 randomly chosen 10 day forecasts are discussed. Since the iteration scheme gives an improved representation of the physics in the atmospheric model, in Section 5 we recommend introducing it operationally.

2. STABILITY ANALYSIS

In this section we start with a simple evolution equation for, say, the temperature of a layer with clouds, which will be discretised along the lines of the ECMWF integration scheme for physics. Then, using the tools provided in the context of one-dimensional maps, we present a qualitative analysis which explains the occurrence of oscillation and noise in parameters such as the temperature and associated heat flux.

Consider a layer with clouds which is surrounded by an infinite' heat bath of fixed temperature T_o. The temperature in the layer is then determined by a balance of input of heat by the sun, radiative cooling and exchange of heat with the surroundings by turbulent diffusion. Disregarding advection, the heat balance in the layer becomes

$$\frac{\partial T}{\partial t} = D - \varepsilon T^3 - k(T - T_o) \qquad (1)$$

where the eddy viscosity depends nonlinearly on $T - T_o$,

$$k = k_o|T - T_o|^m$$

while D represents forcing by the sun and other means and εT^3 represents radiative cooling (with ε a measure for the emissivity). For simplicity here we take $\varepsilon = 1$, and $T_o = 1$.

At initial time the forcing $D = 1$ so that the equilibrium temperature $T = 1$, and the turbulent heat flux vanishes. After 5 time steps the forcing drops by 25% (because the sun goes down) giving a slightly reduced temperature of the cloud layer. The exact solution for two eddy viscosities ($m = 1$ and $m = 4$) is shown in Fig 3.

We discretize Eq (1) by writing for the turbulent layer

$$q = k \times (T - T_o) = k[\beta(T_{n+1} - T_o) + (1 - \beta)(T_n - T_o)] \tag{2}$$

where the subscript refers to the time level and β is chosen to be $\beta = 1.5$ in agreement with the value taken in the ECMWF integration scheme. As a result we find with

$$S_n = D - \varepsilon T_n^3 - k_n(T_n - T_o) \tag{3}$$

that

$$T_{n+1} = T_n + \Delta t \frac{S_n}{1 + \beta k_n \Delta t} \tag{4}$$

Results of the numerical scheme (4) for $m = 1$ and $m = 4$ are shown in Fig.3 as well and they reveal oscillatory behaviour. As will be seen below, these oscillations appear because the equilibrium solution (which will be referred to from now on as a fixed point) is unstable according to the numerical scheme.

In order to try to understand the occurrence of these oscillations (or 'noise') in the solution for temperature and also the turbulent fluxes, we study properties of the one-dimensional map

$$x_{n+1} = f(x_n; \lambda) \tag{5}$$

where for the present scheme

$$f = x_n + \Delta t \frac{S_n}{1 + \beta k_n \Delta t}$$

with

$$S_n = D - \varepsilon x_n^3 - k_n(x_n - x_o)$$

and

$$k_n = k_o|x_n - x_o|^m$$

We study some properties of the mapping f with fixed β while the parameter $\lambda(= \Delta t$, the numerical time step) is varied. It is assumed that the fixed point of the continuous system is stable, while we also assume that the fixed point of the discrete system coincides with the one from the continuous system. Furthermore, we assume that there is a finite neighbourhood around $\lambda = 0$ for which the fixed point remains stable. The following analysis will be illustrated by Figures that result from the simple example with $\varepsilon = 0, k_o = 1, m = 4$ and $x_o = 0$, hence

$$S = 1 - |x|^4 x \tag{6}$$

but the conclusions apply to any mapping which has an extremum in a finite interval (there is also an additional condition involving the so-called Schwarzian derivative of f, but this condition is not very restrictive).

Let us denote the fixed point of f by x_*, thus

$$x_* = f(x_*)$$

and the question of stability of the fixed point may be answered by means of the usual linear stability analysis. Hence

$$x_{n+1} = x_* + \delta x_{n+1}$$

where $\delta x_{n+1} << 1$ and linearising Eq.(5) gives

$$\delta x_{n+1} = \frac{d}{dx}(f)\delta x_n$$

Therefore, we have stability when

$$\left|\frac{d}{dx} f(x_*)\right| < 1 \tag{7}$$

since $\delta x_{n+1} \to 0$ for $n \to \infty$. Suppose that the fixed point x, becomes unstable if the bifurcation parameter $\lambda = \lambda_1$ (For our simple example $x_* = 1$ and $\lambda_1 = 1$). What happens next is illustrated in Fig 4. Since for $\lambda > \lambda\varepsilon_1$ there is no attracting fixed point, the solution will become time dependent and it turns out that instead of having a solution with period 1 (which corresponds to the fixed point) the system has a stable cycle of period 2; hence, the cycle contains two points. These two points turn out to be fixed points of the function f^2 (applied twice), as is illustrated in Fig 4 for $\lambda = 1.25$.

Remark:

If the function f has a fixed point then the function f^n (f applied n times) also has as fixed point x. When x is marginally stable, $|df(x_*)/dx| = 1$, then at $x = x_*$ the slope of f^2 is just 1 (cf. Fig 4a).

In the unstable regime, the slope of f^2 at x_* is bigger than 1, therefore possibly two new fixed points of f^2 are born as is illustrated by Fig 4b

It is now clear that a recurring pattern occurs. The nontrivial fixed points of f^2 (denote them by x_1 and x_2) may also become unstable since the slope of f^2 at x_1 and x_2 may become larger than 1 for a certain value of $\lambda = \lambda_2$. For $\lambda > \lambda_2$ another period doubling occurs as follows from the observation that the function f^4 gets a number of nontrivial fixed points (cf. Fig 4c and 4d). Feigenbaum has shown that this process of successive period doubling continues with the range of parameter values for which the period remains fixed, becoming smaller and smaller until at a certain value of the bifurcation parameter the solution becomes aperiodic, and therefore chaotic. This analysis offers, therefore, an explanation for the occurrence of noise in, for example, the ECMWF integration scheme for physics. In fact, we have explained the occurrence of the oscillations using one of the standard routes to chaotic behaviour. No matter how interesting the subject of chaos is, it should be emphasised that in this case the occurrence of chaos is entirely spurious since the continuous system has the simple behaviour of a stable fixed point. It is simply an artefact of having an unstable numerical scheme.

3. SUGGESTIONS FOR AN IMPROVED NUMERICAL SCHEME

From the above analysis it is clear that one should introduce a numerical scheme that avoids the spurious aperiodic behaviour and a secure way to do this is to use a scheme that always has a stable fixed point. A practical scheme that meets this requirement is what we will call the linearised Crank-Nicholson scheme. This scheme has been used in the WAM model since 1985 *(Komen et al.*, 1994).

Choose as starting point the dynamical equation

$$\frac{\partial x}{\partial t} = S(x) \tag{8}$$

According to Crank-Nicholson a stable scheme is

$$x_{n+1} = x_n + \Delta t[\alpha S(x_{n+1}) + (1-\alpha)S(x_n)] \tag{9}$$

with $\alpha > ½$. In general S is nonlinear so that it is not straightforward to obtain an explicit expression for x_{n+1}. It is therefore customary to linearise S around x_n

$$S(x_{n+1}) = S(x_n) + (x_{n+1} - x_n)\frac{\partial S}{\partial x_n} + \ldots$$

Disregarding the quadratic terms on finds

$$x_{n+1} = x_n + \frac{\Delta t S(x_n)}{1 - \alpha \Delta t \frac{\partial S}{\partial x_n}} \tag{10}$$

If S allows a stable fixed point, $\partial S(x_*)/\partial x<0$, then it may be shown that the numerical scheme (10) is stable provided $\alpha>½$. The proof of this is as follows. First of all observe that if the continuous system has a fixed point also the discrete system (10) has the same fixed point. The fixed point is stable if at $x = x_*$, $|g'| < 1$ where the map g is given by

$$g = x + \frac{\Delta t S(x)}{1 - \alpha \Delta t \frac{\partial S}{\partial x}}$$

and the slope of g at the fixed point $x = x$, becomes

$$\frac{\partial g(x_o)}{\partial x} = 1 + \frac{\Delta t \frac{\partial S}{\partial x}}{1 - \alpha \Delta t \frac{\partial S}{\partial x}}$$

since $S(x_*) = 0$. Hence, we have marginal stability for $|g'(x_*)| = 1$, which reduces to the condition

$$1 - 2\alpha = -\frac{2}{\Delta t \frac{\partial S}{\partial x}} \tag{11}$$

Since the continuous system has a stable fixed point, $\partial S/\partial x<0$ at $x = x_*$, the scheme (10) is stable provided $\alpha>½$ because the marginally stable condition (11) cannot be met.

Therefore, the linearised Crank-Nicholson scheme (10) with $\alpha>½$ seems to be a promising alternative. In fact, the exact solutions displayed in Fig 3 were obtained with this numerical scheme.

In passing, we note that the reason for the oscillations in the present ECMWF scheme is that the implicit factor, as given in for example Eq (4), viz $\beta k \Delta t$, is just a poor approximation to the factor that is really needed in a stable scheme, namely $-\alpha \Delta t(\partial S/\partial x_n)$. Only when the eddy viscosity is a linear function of x, and only when the remainder of the source term depends weakly on x can one expect the EC scheme to be stable (note that typically $\beta = 2\alpha$). In cases when the eddy viscosity depends in a nonlinear way on, or when the remainder of the source function S depends sensitively on x, the EC scheme will become unstable giving oscillatory or even aperiodic solutions.

It should be emphasized, however, that the linearised Crank-Nicholson scheme requires the determination of the derivative of the source functions of both physics and dynamics. This information could be provided by the tangent-linear of the model or $\partial S/\partial x$ could be determined explicitly as is done in the WAM model, for example. In any case this requires a considerable amount of effort.

An alternative approach, which has been well tested is to apply the usual ECMWF integration scheme for vertical diffusion n times with a time step of $\Delta t/n$. Although this approach does not guarantee stability of the fixed point, it makes it more unlikely that instability occurs. Also in the case of a stable fixed point (as, for example, happens for momentum transfer) the iteration approach gives a more accurate solution. Consider, for example, a case where the initial value of $x = x_o$ is

far away from the fixed point x_*. Suppose that the relaxation time for physical processes is very short. In that event, one would expect a very rapid transition from $x = x_0$ to the steady state value x_*. The standard EC scheme would however show a considerable overshoot (or undershoot) because the integration time step Δt is much larger than 1. Using the iteration approach one may avoid overshoot provided the integration time step is reduced sufficiently. In practice, it turned out that a reduction of physics time step by a factor of 3 was sufficient to remove over- or undershoot.

In order to illustrate the higher accuracy of the iteration scheme, we return to Fig 1 where we have also shown the dependence of drag coefficient on wind speed when the semi-implicit integration scheme is applied three times with a time step $\Delta t/3$. Comparing the simulated drag with the one for the Charnock relation it is clear that in that case a considerable reduction in scatter occurs while for high winds the underestimation of drag disappears.

Because of the smaller time step the iterative semi-implicit scheme is also able to suppress oscillations in the fluxes as shown in Fig 2. Finally, the iterative scheme ($n = 3$) was also applied to the cases discussed in Fig 3 and results were almost identical with the exact solution.

We therefore thought that the iterative semi-implicit numerical scheme offers a viable option towards a more accurate representation of the physics in an atmospheric model. In the next section we discuss the possible impact of such a scheme in a GCM at several resolutions and time steps.

4. APPLICATION OF AN ITERATIVE, SEMI-IMPLICIT SCHEME

In this section we briefly discuss some results of the application of the iterative numerical scheme to a case of an extreme low, to 10 day weather forecasting and to simulation of the seasonal climate.

4.1 Simulation of the Braer storm

As a demonstration of the alternative approach discussed in the previous section, numerical simulations of the extra tropical cyclone that set a record for the minimum central pressure for the North Atlantic were performed. (The gales associated with this record low severely damaged the oil tanker Braer, hence the name Braer storm). The T106 version of the ECMWF model with 31 vertical levels was used. The model was initialised with data from the ECMWF reanalysis for 1200 UTC 9 January 1993, which is 24 h prior to rapid cyclogenesis.

The cyclone of interest, located to the southeast of Iceland in the T106 control simulation, attains a remarkably deep central pressure of 919 hPa after 24 h, as shown in Fig 5a. A second simulation, referred to as VDIF, was performed with a model configuration that was identical to the control except that the vertical diffusion parametrization has a time step that is three times smaller than the control simulation. The 24 h sea-level pressure field is shown in Fig 5b. Although the character of the two simulations is quite similar, the central pressure in VDIF is deeper by 0.5 hPa, which is in slightly closer agreement with the T213 operational mean sea-level pressure analysis for 12 UTC 10 January 1993 (Fig 5c). The maximum difference in sea-level pressure between the control and VDIF is about 1.5 hPa (Fig 5d); the difference pattern suggests a small shift in the location of the low.

In the following 24 h period, the cyclone begins to fill, with a central pressure of 926 hPa at 12 UTC 11 January as indicated in the analysis shown in Fig 6c. Although the northeast Atlantic region is

rather data sparse, the sea-level pressure analysis appears in reasonable agreement with the reporting observations. For example, the surface wind and sea-level pressure observations for 12 UTC 11 January shown in Fig 7, indicate a 925.6 hPa ship observation to the southeast of Iceland. The results for the 48 h sea-level pressure for the control and VDIF experiments are shown in Figs 6a-b, respectively. The simulated sea-level pressures are as much as 1.8 hPa higher near the cyclone centre in the VDIF experiment than the control (Fig 6d), which is once again in closer agreement with the operational analysis (Fig 6c). However, in both experiments the cyclones appear to have a too rapid eastward phase speed relative to the analysis. We also remark that over orography, where a strong forcing of the flow may occur, considerable differences in the surface pressure may be noted, in particular at day 2 of the forecast.

The 31 m wind field for the 48 h time for the control and VDIF experiments, shown in Fig 8a-b, indicates a well defined low-level jet with a near-surface maximum in excess of 32 m/s located over the Norwegian Sea to the west of the Norwegian coast. The VDIF experiment has wind speeds in the centre of the low-level jet that are about 3.5 m/s higher than in the control experiment (Fig 8d). Although both of these simulations have wind speeds that are greater than the analysed wind speed maximum to the north of the United Kingdom (Fig 8c), several surface observations in the North Sea at 12 UTC 11 January (Fig 7) indicate near-surface wind speeds in excess of 30 m/s.

The changes to the vertical diffusion have an impact upon the surface stress as well, as indicated in Fig 9. A well defined surface stress maximum is present to the north of the United Kingdom in the vicinity of the low-level jet in both the control and VDIF experiments (Fig 9a and 9b respectively). The larger near-surface wind speeds in the VDIF experiment result in a 15% increase in the surface stress in the vicinity of the low-level jet for the time period between the 24 and 48 h times, as shown in Fig 9c.

As a general remark, it should be pointed out that both T106 simulations at the 24 h time seem to underestimate the strength of the analysed record low by 6-7 hPa. An obvious explanation is that the simulations have been performed with a too coarse resolution model since the analysis was generated by the T213 version of the atmospheric model. In such an extreme event, resolution will no doubt be an issue. However, a smaller integration time step may affect results as well. In order to illustrate this point we compared results of the T106 model with a time step of 30 minutes with results obtained with a time step of 2 minutes. We performed integrations with the Eulerian version of the atmospheric model since the fully interpolating semi-Lagrangian scheme would give for small time step an excessive smoothing of the relevant fields (Clive Temperton, private communication). A comparison of surface pressure fields from the large and small time step results is given in Fig 10a and 10b, while the difference in pressure is shown in Fig 10c. We remark that the large time step simulation gives a central pressure which is 1 hPa higher than the simulation with the semi-Lagrangian scheme of Fig 5a, but the 2 minute time step simulation with the Eulerian scheme gives a central pressure which is 5 hPa lower, in much closer agreement with the operational analysis of Fig 5c. The pressure difference of Fig 10c shows considerable differences when going to a smaller time step.

It is concluded that in extreme events simulation with the ECMWF atmospheric model shows a considerable dependence on the integration time step. This is partly caused by too large a time step in the physics scheme. In the Braer storm there is, however, also a considerable time step dependence caused by the dynamics.

4.2 Ten day weather forecasting and systematic effects

The impact of the iterative numerical scheme for physics upon routine 10 day weather forecasting was tested by performing 12 randomly selected forecasts using the T106 configuration of the ECMWF model. Despite some significant differences in individual cases such as discussed above, the verification scores indicate that the modified vertical diffusion scheme has on average a relatively minor impact on the large-scale model performance and verification statistics. However, as shown in Fig 11, the new integration scheme had an impact on systematic errors in parameters such as the dry bulb temperature in the tropical area.

A tentative explanation of the impact on systematic errors is as follows: The three-dimensional model results show problems with spurious oscillatory behaviour similar to the one-dimensional model results discussed previously. For example, a time series of model simulated temperature near the top of a cloud layer from grid point in the T106 control simulation is shown by the solid line in Fig 12. Though the oscillation amplitude is rather small in this particular example, this behaviour is obviously not desirable. The iterative scheme for the vertical diffusion, shown by the dashed line in Fig 12, results in the elimination of the spurious oscillation, and on average the mean temperature changes (in this example it is higher). In Section 2 we have seen that the oscillation arises because of instability of the fixed point in the numerical scheme. As a result, the solution and the associated fluxes start to execute an oscillation. However, the mean value of the oscillating quantities does not necessarily coincide with the fixed point as is evident from Fig 4b, 4c and also the one-column results of Fig 2*. As a consequence, by suppressing the 'noise', a more accurate integration scheme may have impact on systematic errors.

We thought therefore it was of interest to perform a few 120 day runs in order to see whether there was evidence of any systematic differences between the control run and the iterative scheme (with 3 iterations). Fig 13 shows the mean 850 hPa temperature (over the last 90 days) for the JJA season of 1987 for the control, the modified vertical diffusion scheme and their differences. Considerable differences in temperature are seen over North America, Russia and North Africa. The increase in temperature as found with the iterative scheme was also noted in a 120 day run in which the integration time step for both dynamics and physics was reduced by a factor 3, Fig 14. Because of the large variability in the extra-tropics we repeated the 120 day runs for different initial conditions and a similar picture emerged. This, therefore, suggests that the iterative scheme gives more accurate results regarding temperature. Finally, the iterative scheme also had a considerable impact on the zonal mean of the zonal wind during the Southern Hemisphere winter as is shown in Fig 15. At the jet level increases in mean wind speed of about 10% are seen while near the surface the mean wind speed is larger by 3 m/s which is considerable. Nevertheless, because of the large variability during the winter season the results for wind speed should be interpreted with care.

It is therefore concluded that the iterative integration scheme for physics may have a considerable impact on the systematic errors of the atmospheric model.

*. Note that this may be regarded analogous to wave-mean flow interaction occurring for example in Rossby waves.

5. CONCLUSION

We have attempted to explain the occurrence of numerical noise in the ECMWF atmospheric model by studying properties of one-dimensional maps, which may be regarded as a metaphor for a numerical integration scheme. For a large enough numerical time step the fixed point of the maps (corresponding to the physical steady state) becomes unstable and an oscillation with period 2 is born. Further increase of time step results in successive period doublings until at a certain critical value of the time step aperiodic, chaotic behaviour is found. This chaotic behaviour explains the occurrence of noise but is entirely spurious because it is a property of the discretised system and not of the underlying physics.

Suggestions for avoiding this spurious chaotic behaviour are given. A good candidate for a numerical scheme seems to be the linearised Crank-Nicholson scheme. As soon as the tangent linear model is available it is recommended to start to do experiments with this scheme. Alternatively, one could explicitly introduce the determination of the relevant derivatives of the (Physics) source terms. For the moment, we have to fall back on iterating the physics several times. Extensive testing of the iteration scheme shows that it behaves well in extreme conditions with respect to, for example, the consistency between wind speed and stress. Also the numerical noise is suppressed by this scheme. It is therefore recommended to introduce the iterative integration scheme operationally.

ACKNOWLEDGEMENT

We gratefully acknowledge useful discussion with Anton Beljaars, Jan Barkmeijer, Christian Jakob, Jean-Jacques Morcrette, Jean-François Mahfouf and Pedro Viterbo.

REFERENCES

Feigenbaum, M J, 1980: Universal behaviour in nonlinear systems, Los Alamos Science 1, 4-27.

Janssen, P A E M, A C M Beljaars, A Simmons and P Viterbo, 1992: On the determination of surface stress in an atmospheric model. Monthly Weather Review 120, 2977-2980.

Komen, G J, L Cavaleri, M Donelan, K Hasselmann, S Hasselmann and P A E M Janssen, 1994: Dynamics and modelling of ocean waves, Cambridge University Press, 532 p.

Ritchie, H, C Temperton, A Simmons, M Hortal, T Davies, D Dent and M Hamrud, 1995: Implementation of the semi-Lagrangian method in a high-resolution version of the ECMWF forecast model, Monthly Weather Review, 123, 489-514.

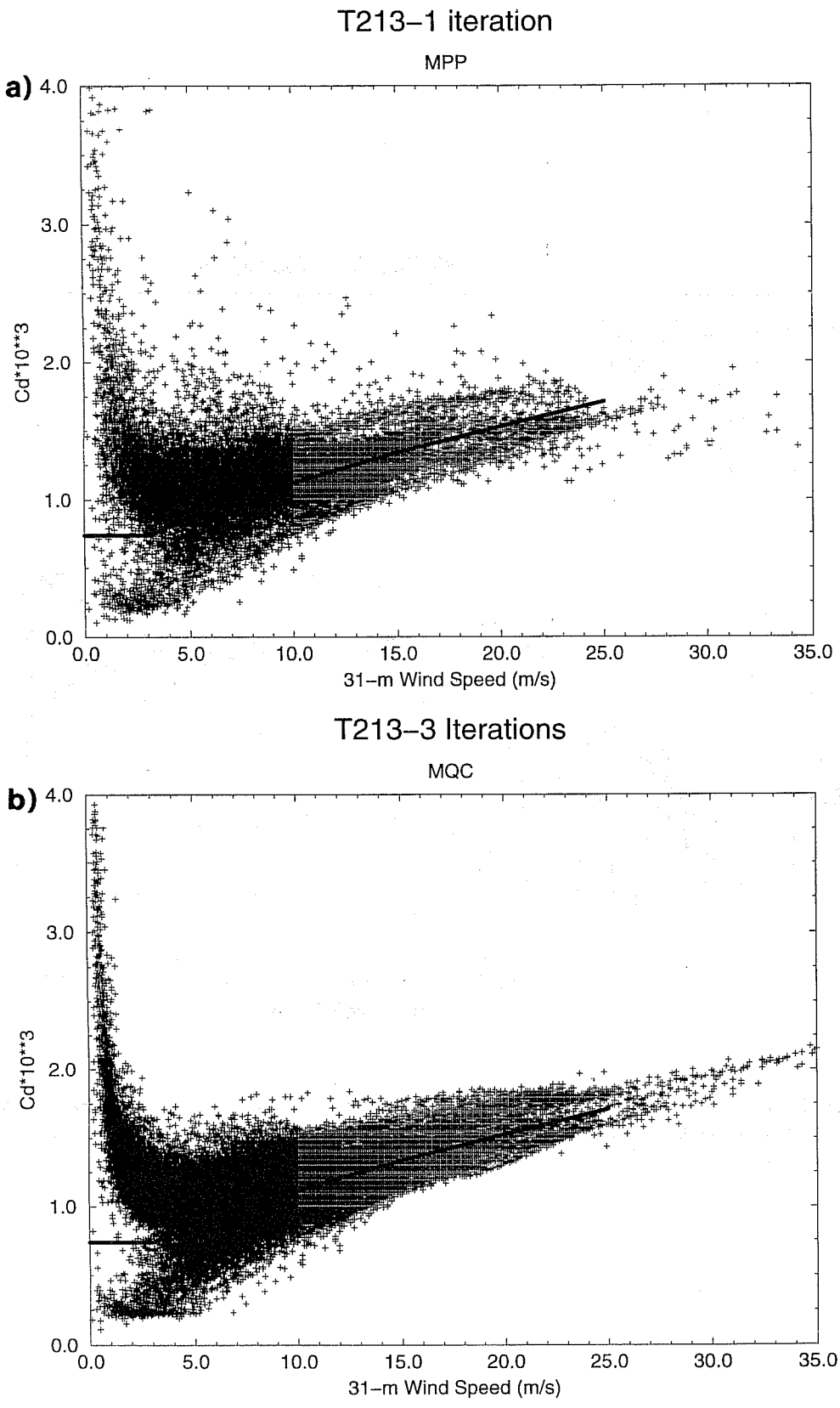

Fig. 1: a) Drag coefficient versus 31 m wind speed with one iteration and b) with 3 iterations. Model is T213/L31 with three time level integration scheme with a dynamics time step of a quarter of one hour.

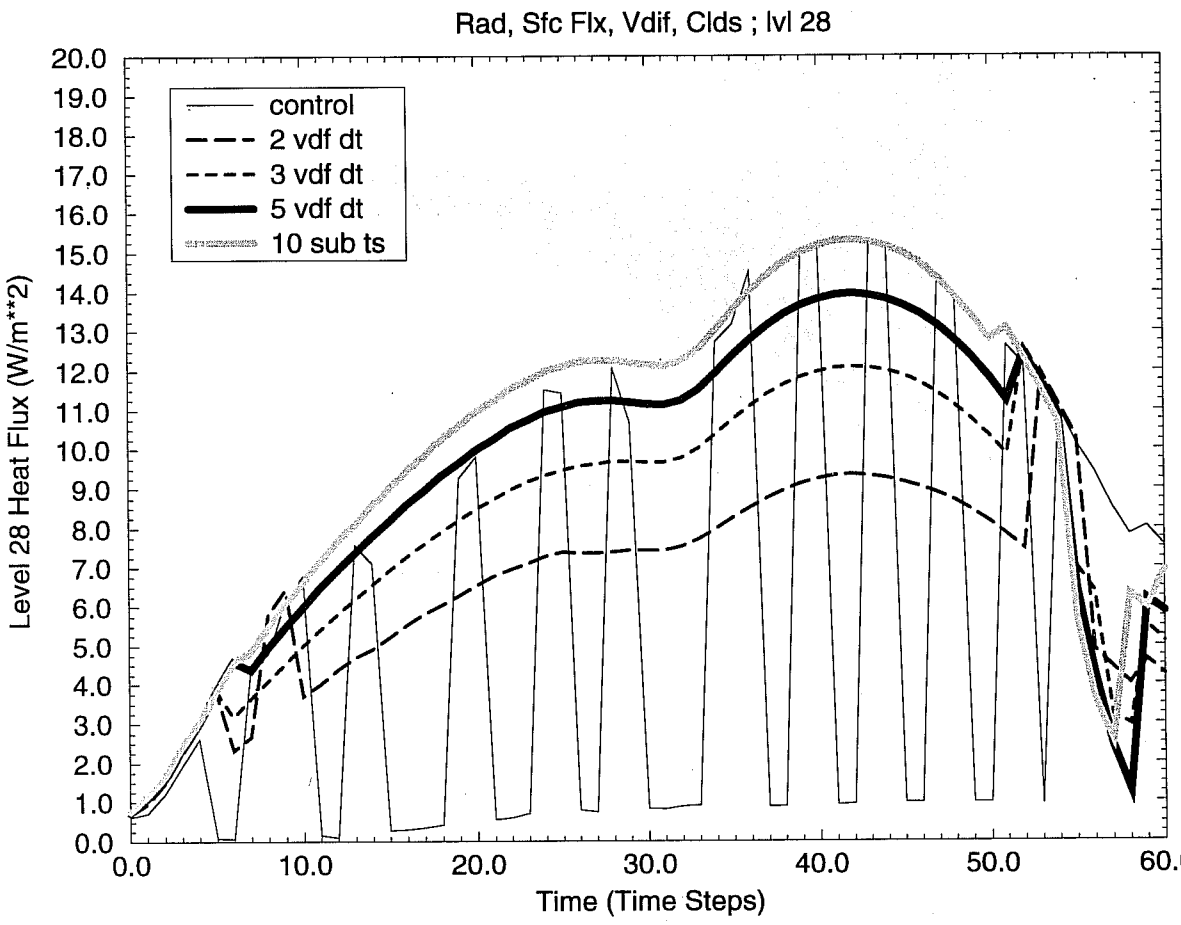

Fig. 2: Results from the one column version of the ECMWF model for head flux at level 28. The "exact" solution is denoted by the grey line. The thin line denotes the solution when vdiff is only called once, while the other line styles denote solutions when vdiff is called 2, 3 and 5 times.

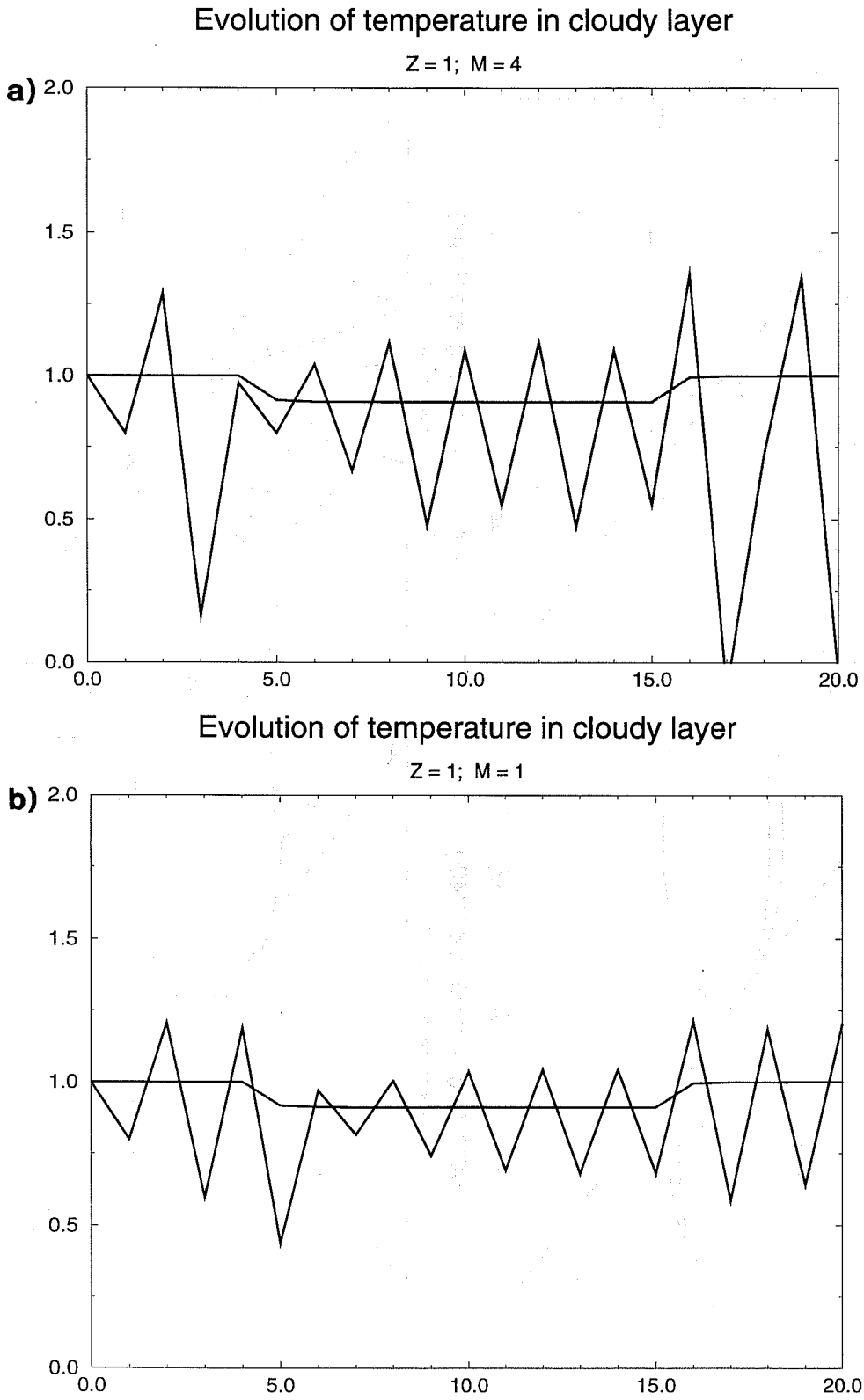

Fig. 3: Evolution of temperature in cloudy layer for a) $\lambda = 1$ and $m = 4$, and b) $\lambda = 1$ and $m = 1$. The line without the oscillation is the exact solution while application of the EC physics scheme gives oscillatory behaviour.

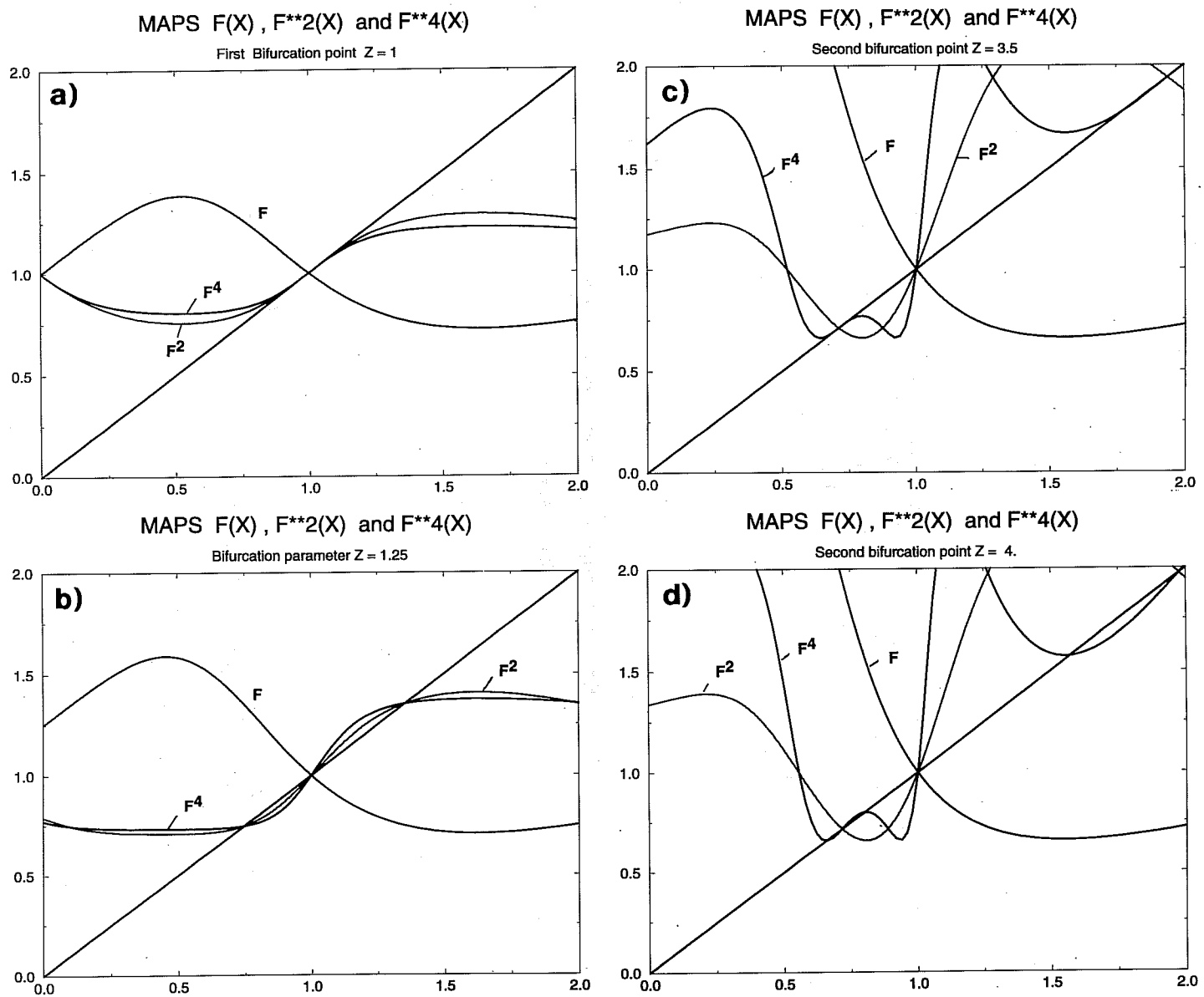

Fig. 4: Maps of f, f^2 and f^4 for different values of the bifurcation parameter λ. Fig. 4a) shows case of marginally stable fixed point, 4b) shows case of first period doubling with unstable fixed point, 4c) shows case of marginally stable period 2 oscillation while 4d) shows a stable period 4 oscillation.

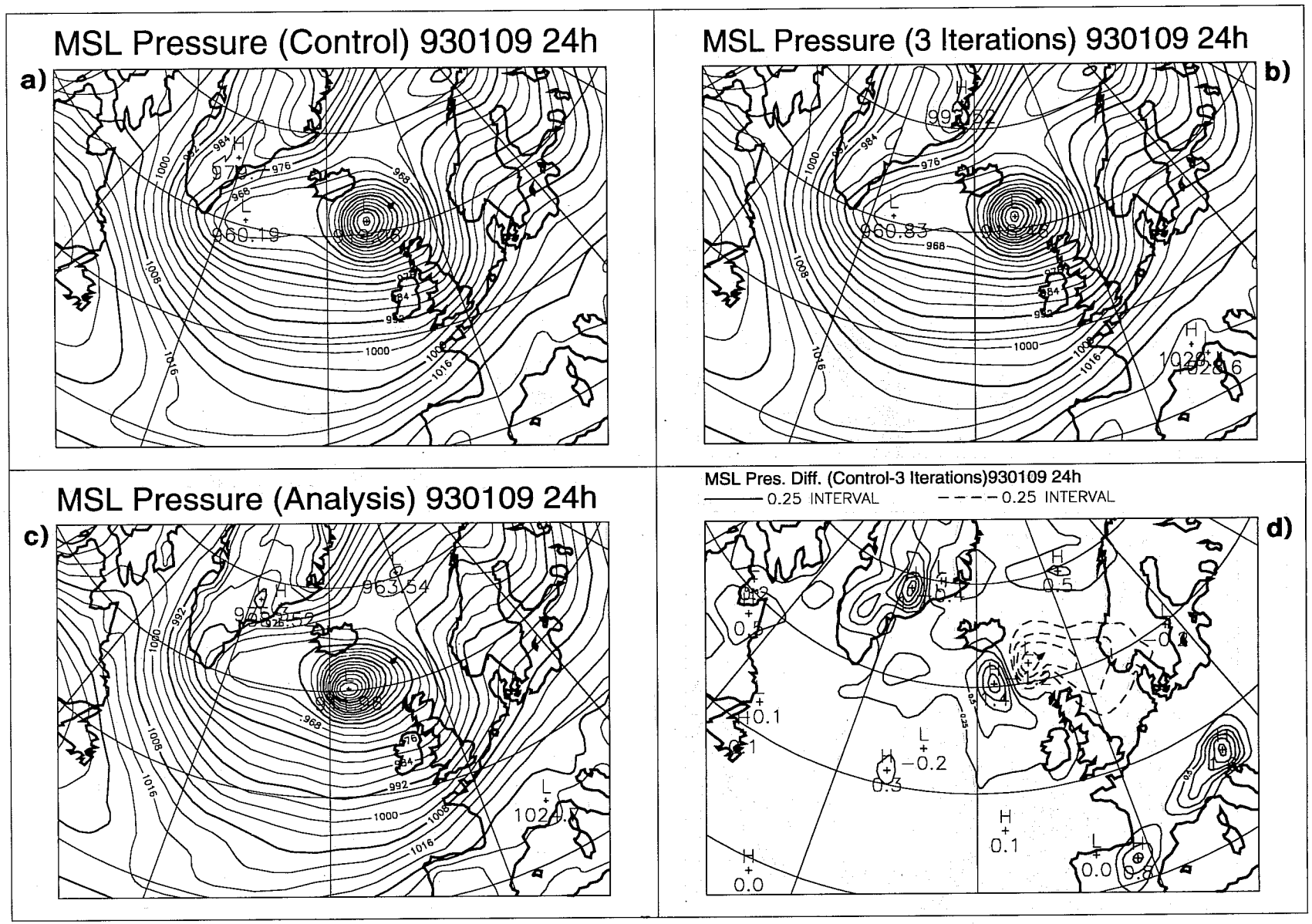

Fig. 5: Surface pressure map in North Atlantic for the Braer Storm. Fig. 5a) shows result from control simulation, fig. 5b) shows the simulation with 3 iterations, fig. 5c) shows the analysis while fig. 5d) shows the difference between 3 and 1 iterations. Forecast at 24 hrs time.

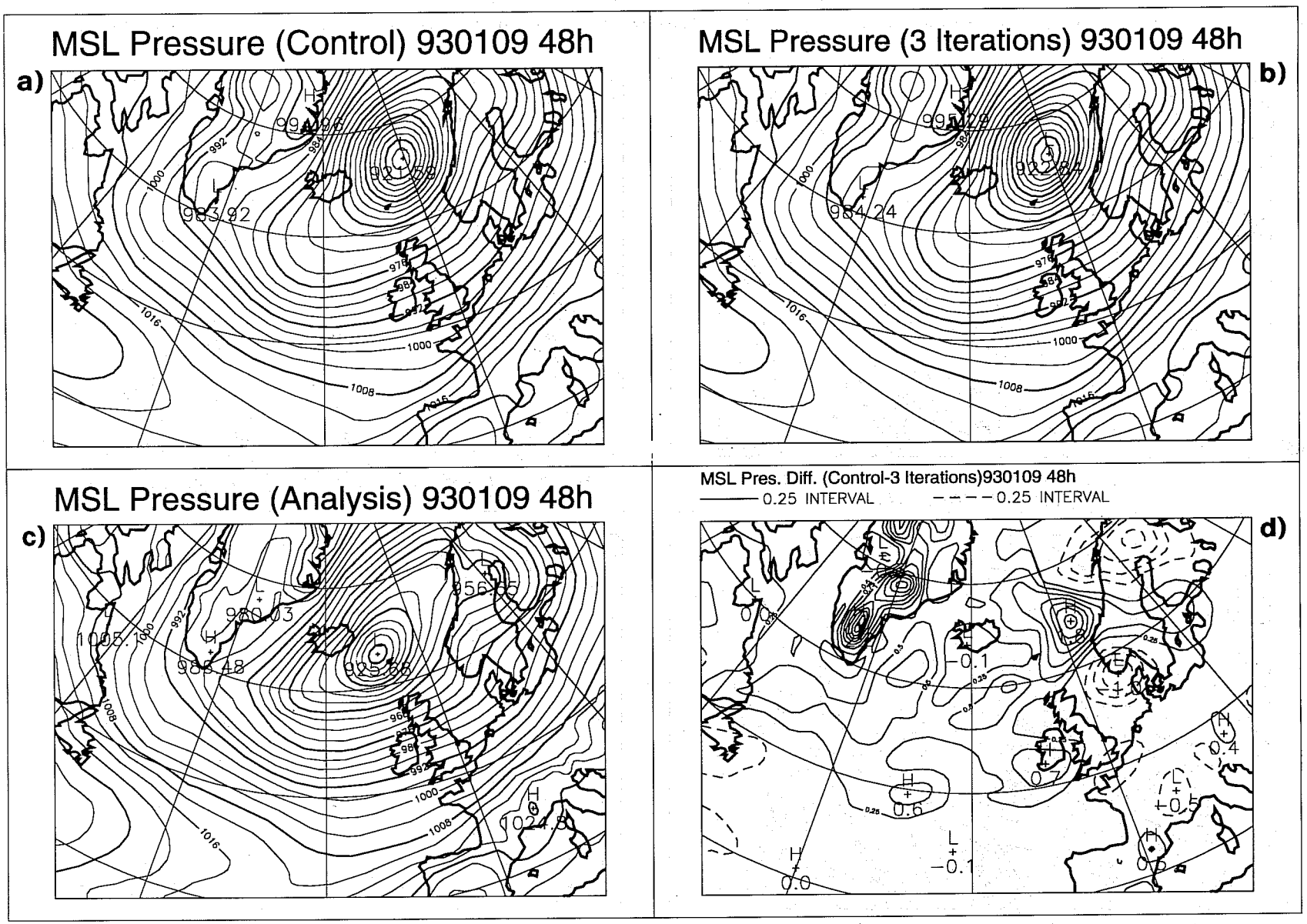

Fig. 6: Idem as Fig. 5 but now at 48 hrs time.

Observations for 93011112

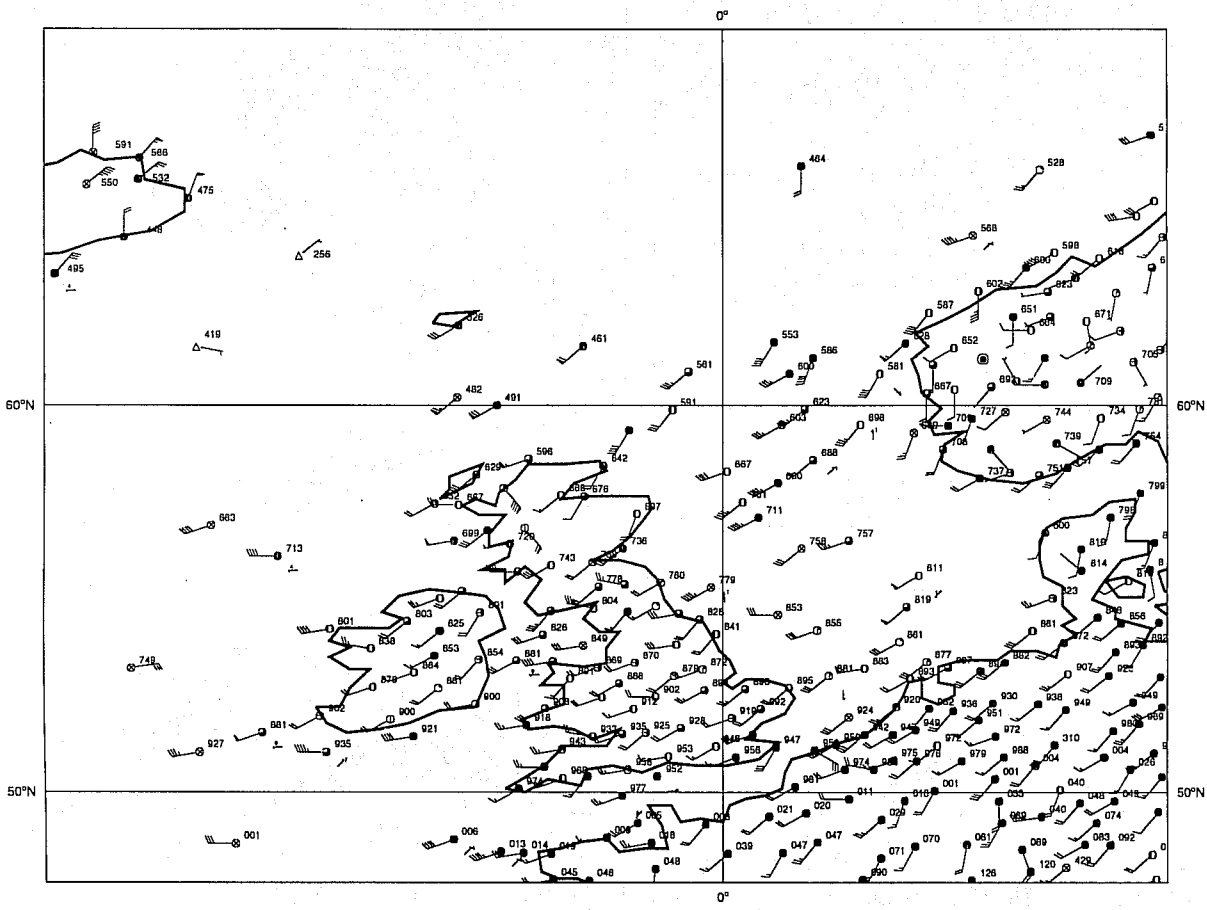

Fig. 7: Surface observations at 11 January 1993 for North Eastern Atlantic

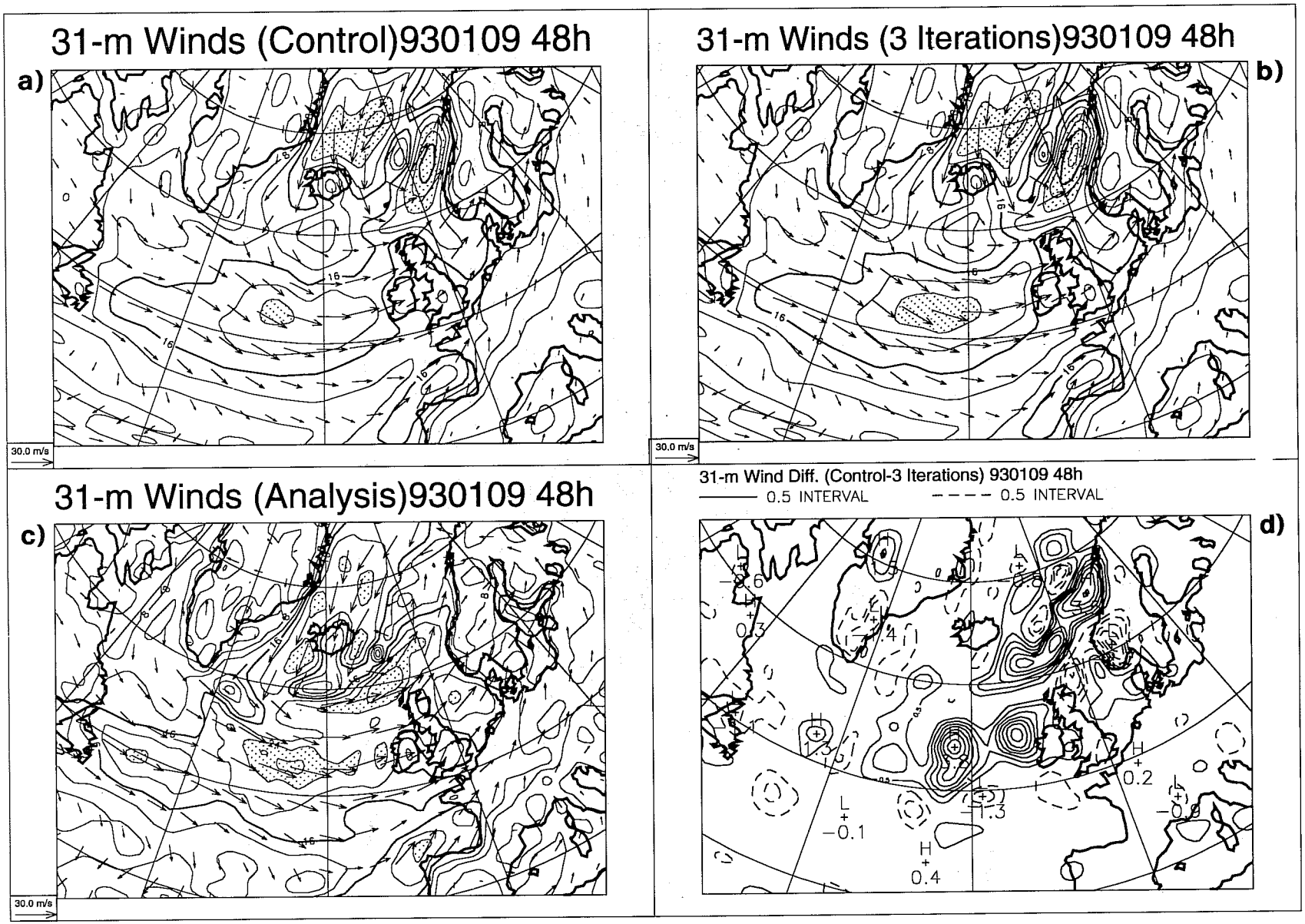

Fig. 8: Wind field map in North Atlantic for the Braer Storm. Panel a) shows control, b) shows results from simulation with 3 iterations, c) shows analyzed winds and d) shows difference between 3 and 1 iteration. Forecast at 48 hrs time.

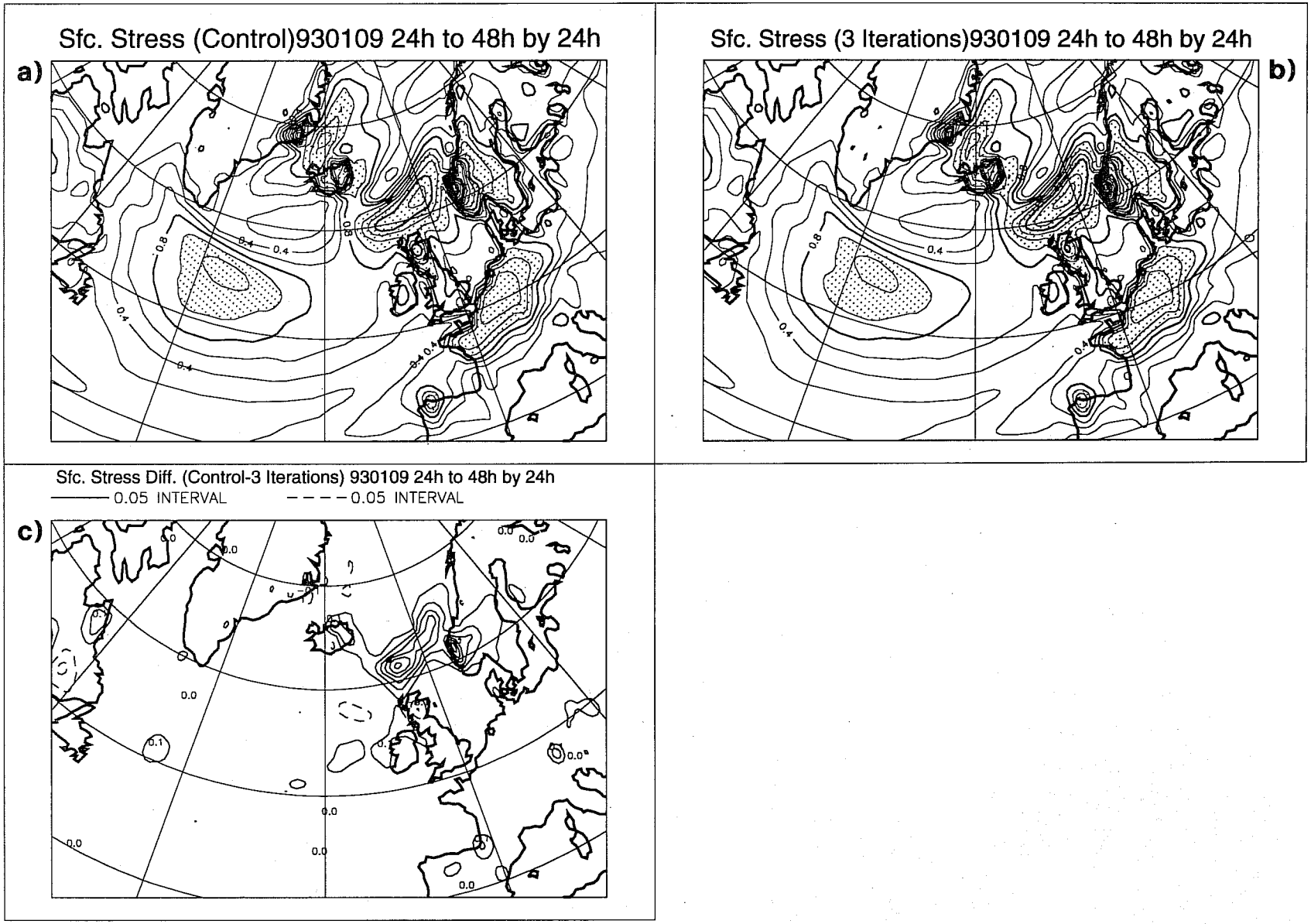

Fig. 9: Daily mean surface stress at 48 hrs time. Panel a) shows control, b) shows 3 iterations result while c) shows the difference between the two.

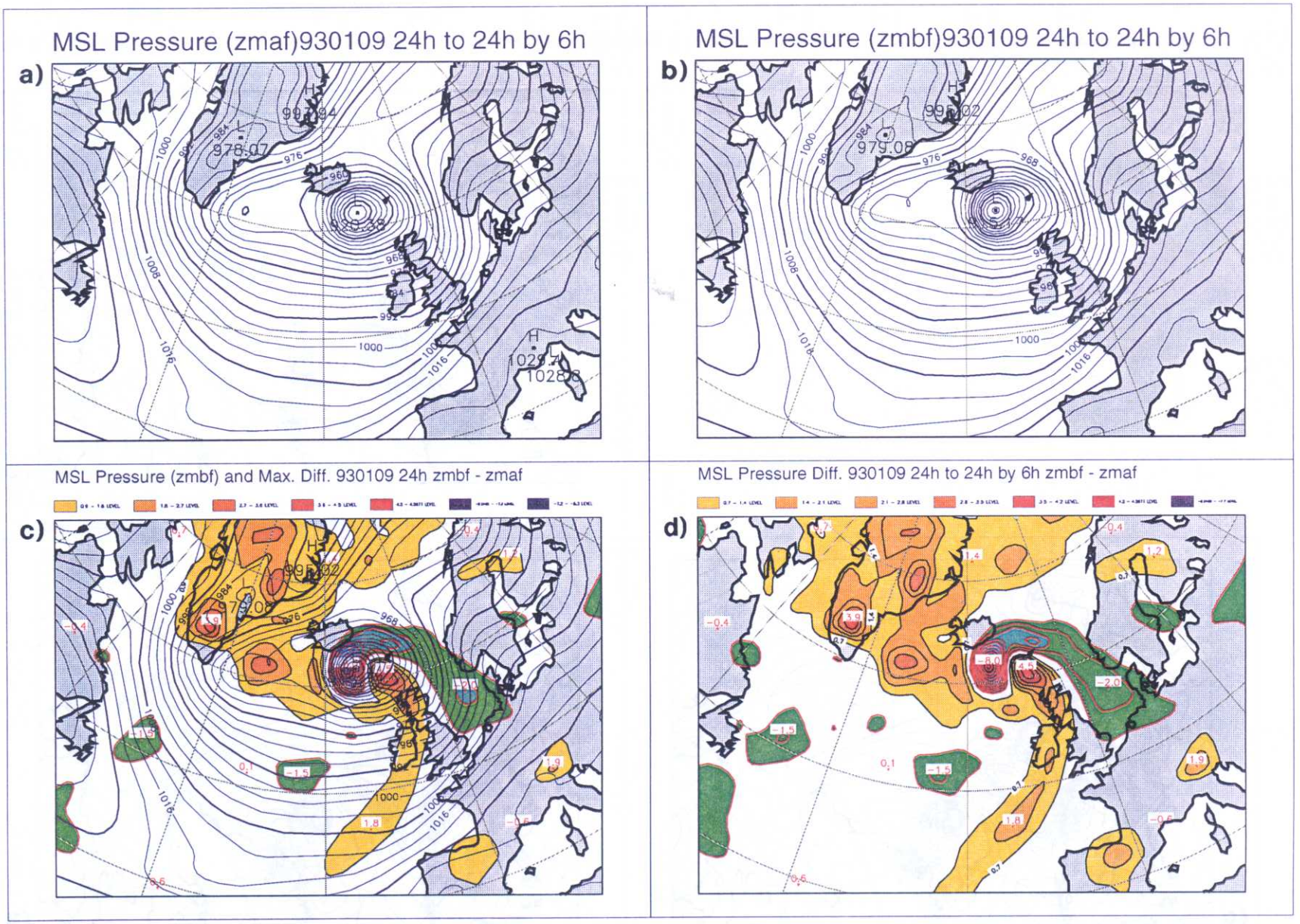

Fig. 10: Simulation of Braer Storm with Eulerian version of T106 - ECMWF model, showing dependence on time step. Panel a) shows simulation with 30 minutes time step, b) shows results with a 2 minutes time step while d) shows the difference between the two.

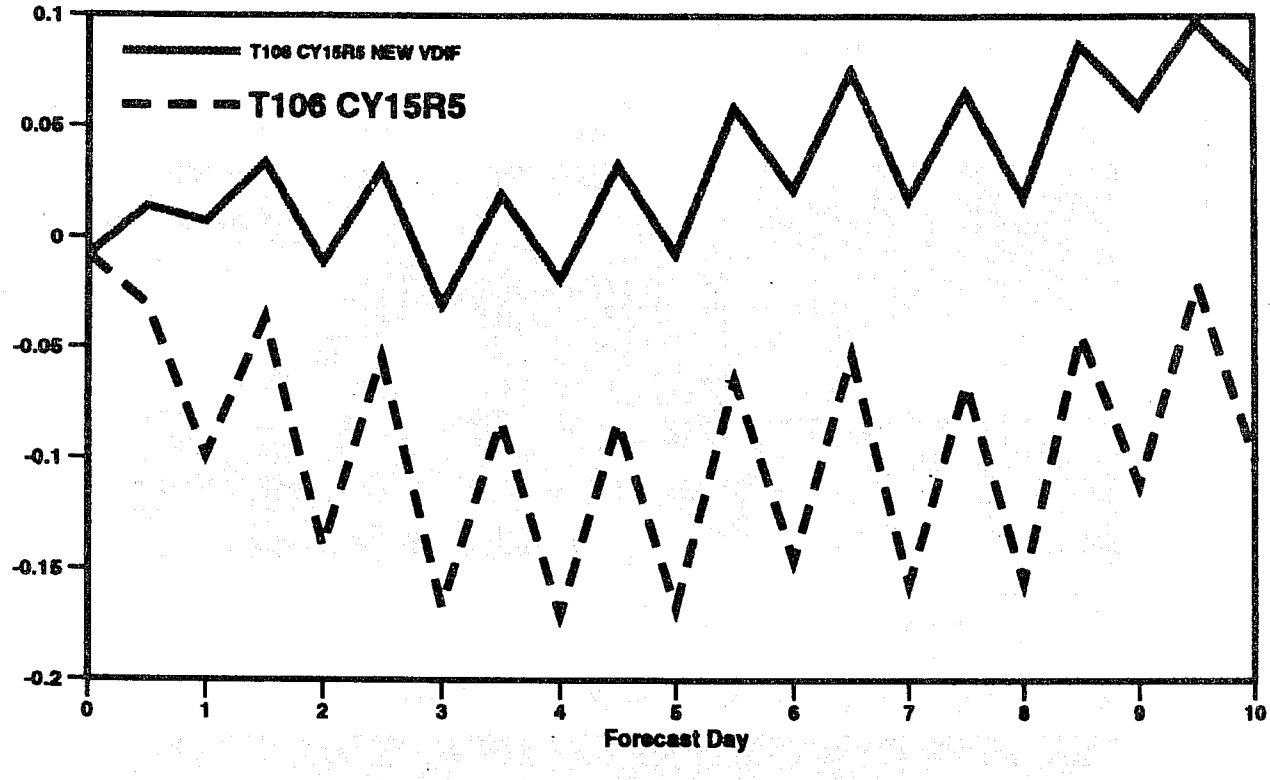

Fig. 11: Impact of iterating vdiff on mean error in temperature during the 10 day forecast in the Tropics. Number of forecasts is 12 and the mean is taken.

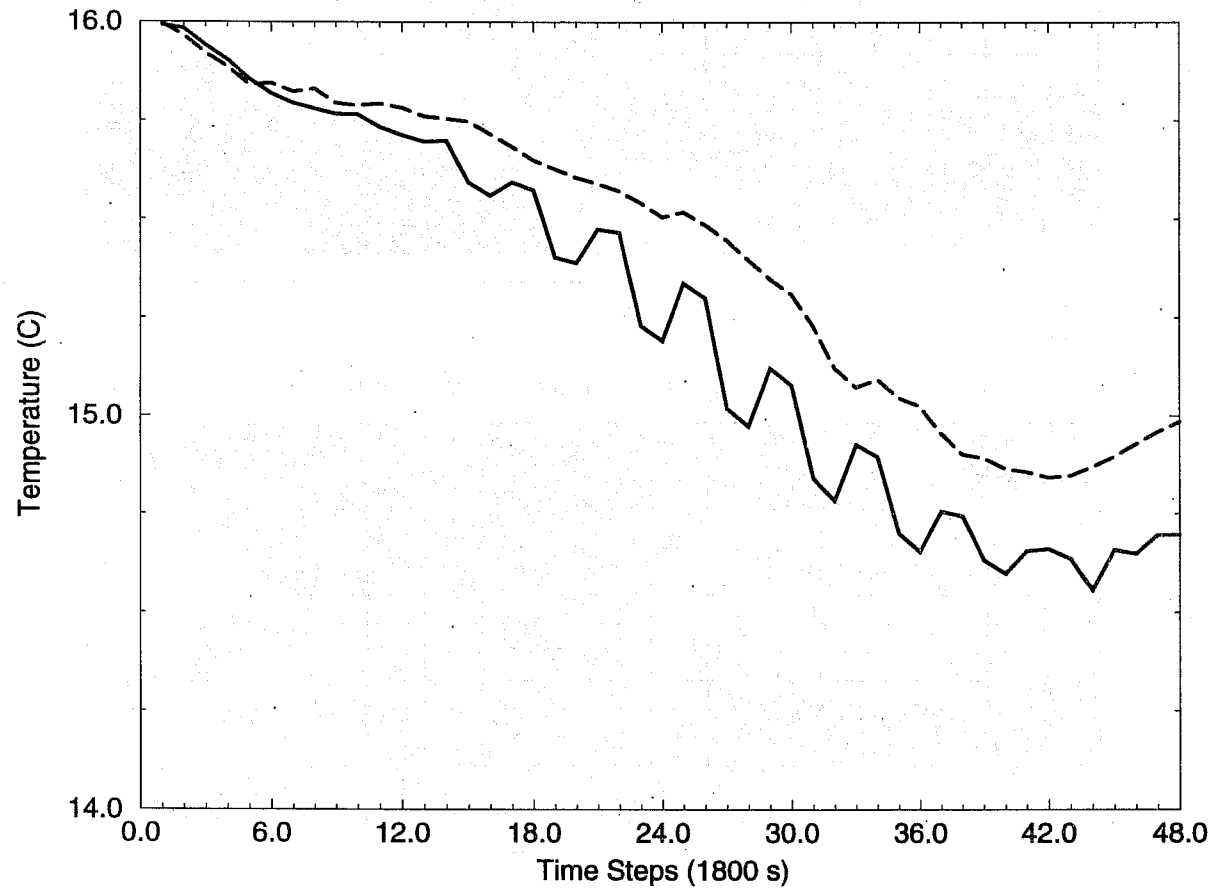

Fig. 12: Evolution of temperature in time for one and three iterations showing a reduction of the oscillations in case of three iterations.

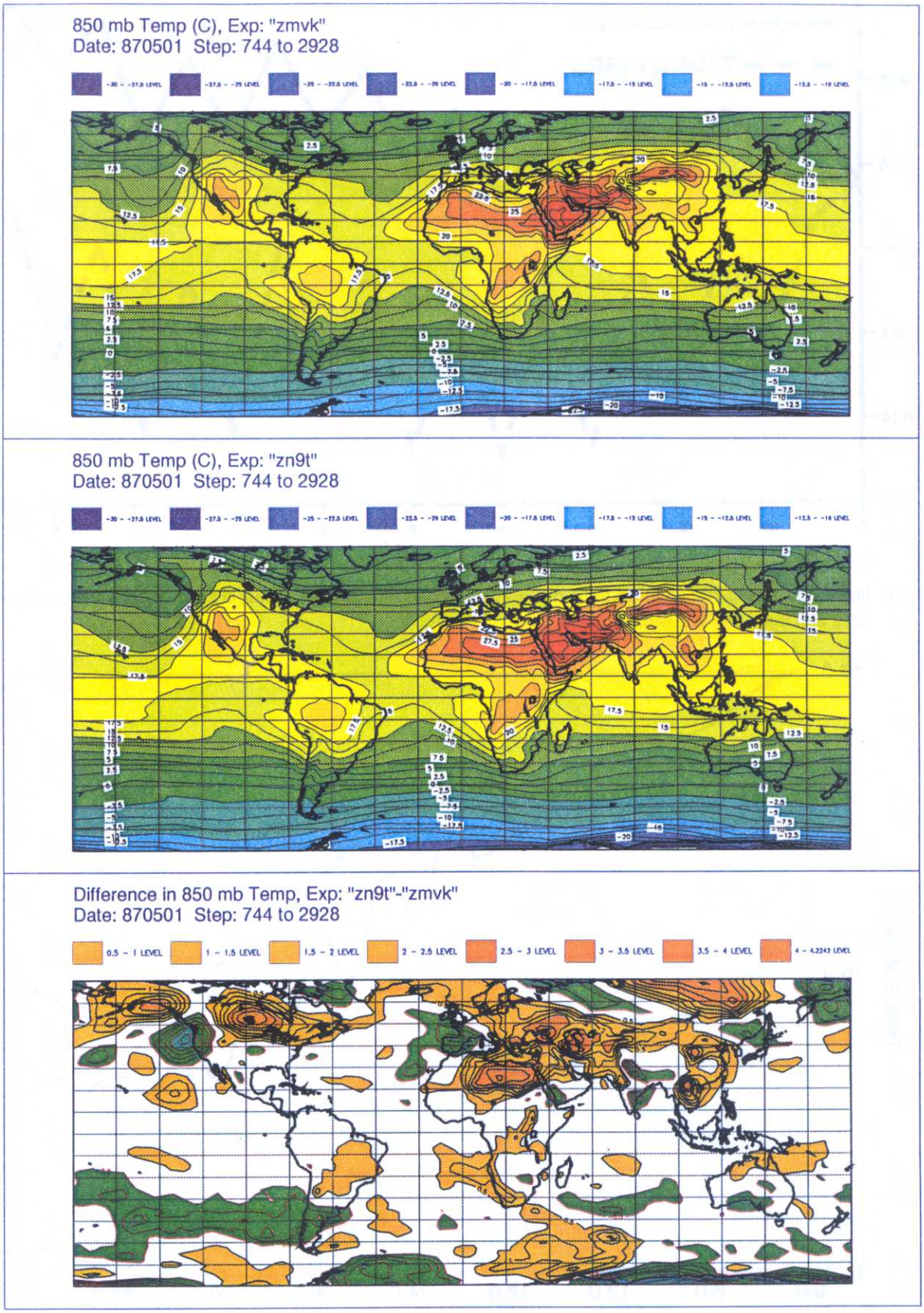

Fig. 13: JJA mean of 850 mb temperature for one and three iterations and their differences.

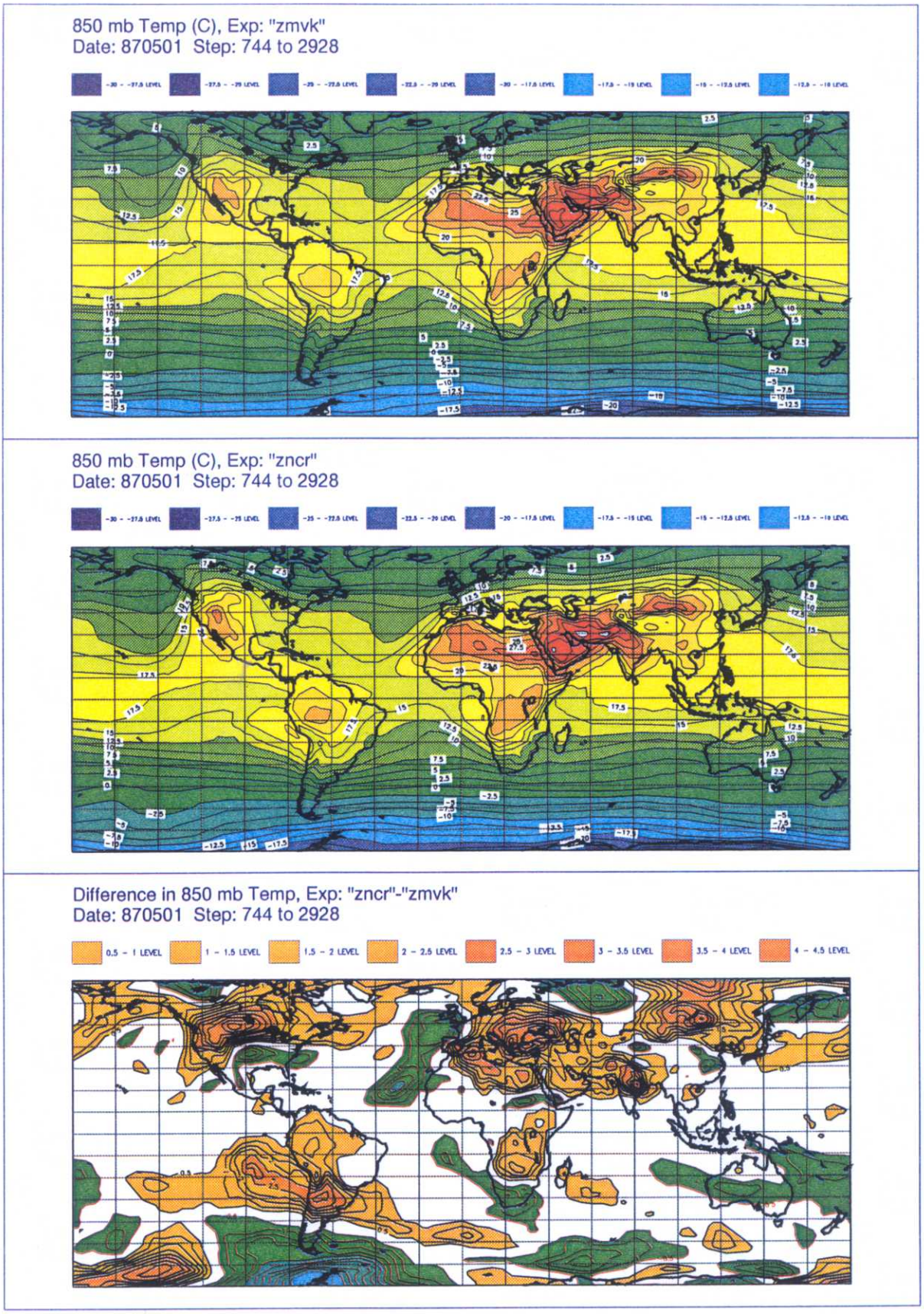

Fig. 14: Time step dependence of seasonal mean temperature field. Exp. "zmvk" is with 30 min time step while "zncr" is with 10 min time step.

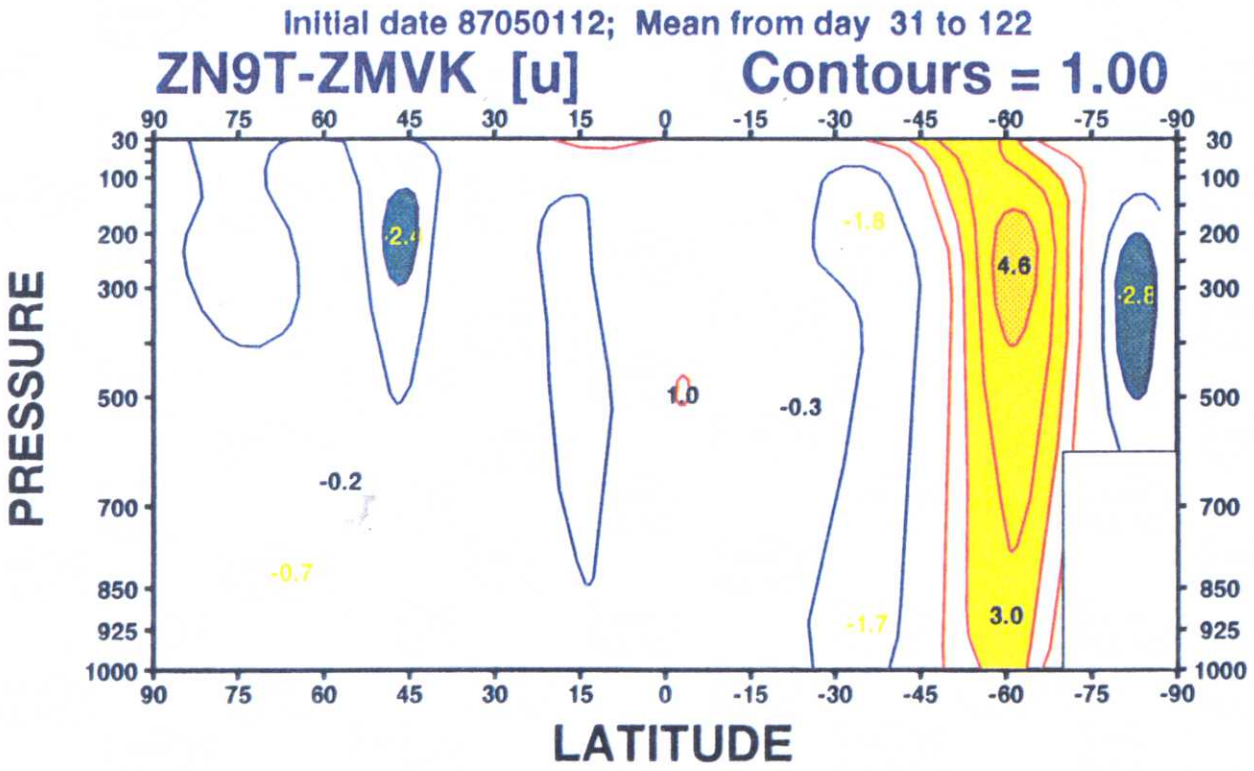

Fig. 15: Cross section of the difference in zonal mean wind for three (zngt) and one (zmvk) iteration(s) for JJA season.